NJC

New Journal of Chemistry

A journal for new directions in chemistry

Accepted Manuscript

This article can be cited before page numbers have been issued, to do this please use: T. Wang, Z. Wang, Z. Pan, A. Dayo , W. Liu and J. Wang, *New J. Chem.*, 2020, DOI: 10.1039/D0NJ04262E.

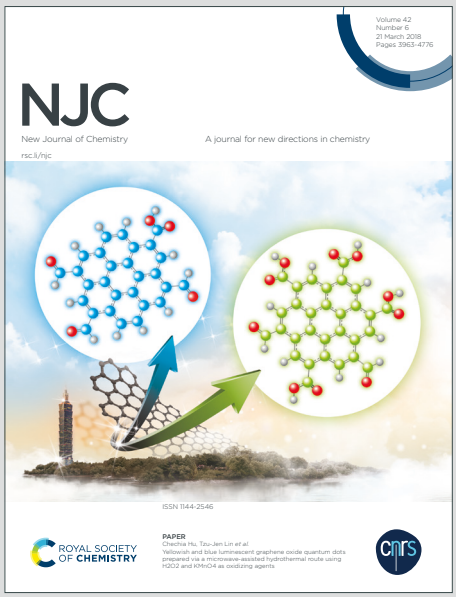

This is an Accepted Manuscript, which has been through the Royal Society of Chemistry peer review process and has been accepted for publication.

Accepted Manuscripts are published online shortly after acceptance, before technical editing, formatting and proof reading. Using this free service, authors can make their results available to the community, in citable form, before we publish the edited article. We will replace this Accepted Manuscript with the edited and formatted Advance Article as soon as it is available.

You can find more information about Accepted Manuscripts in the Information for Authors.

Please note that technical editing may introduce minor changes to the text and/or graphics, which may alter content. The journal's standard Terms & Conditions and the Ethical guidelines still apply. In no event shall the Royal Society of Chemistry be held responsible for any errors or omissions in this Accepted Manuscript or any consequences arising from the use of any information it contains.

View Article Online
DOI: 10.1039/D0NJ04262E

ARTICLE

Synthesis of novel allylamine-fluorene based benzoxazine and its copolymerization with typical benzoxazine: Curing behavior and thermal properties

Received 00th January 20xx,
Accepted 00th January 20xx

DOI: 10.1039/x0xx00000x

Ting Wang,[a] Zhi-cheng Wang,[a] Zhong-cheng Pan,*[a] Abdul Qadeer Dayo,[b] Wen-bin Liu,*[a] and Jun Wang*[a]

In this paper, 2,7-dihydroxy-9,9-bis(4-aminophenyl)-fluorene monomer (BADHF) was synthesized by direct condensation reaction catalyzed by methylsulfonic acid. A novel allylamine-based benzoxazine monomer containing fluorene group and polymerizable group (*t*-BF-sa-a) was obtained via o-hydroxy-benzyl amine method combining with one stage Mannich condensation reaction. The result showed that the introduction of fluorene rings and polymerizable groups and the increase of oxazine rings in the polymer network structure can result in an obvious increase in the crosslinking density of polymers. Therefore, the *t*-BF-sa-a polybenzoxazine (poly(*t*-BF-sa-a)) exhibited a higher glass transition temperature (T_g) and better thermal stability.

The synthesized *t*-BF-sa-a monomer was used to modify traditional phenol-aniline-based mono-functional phenol-aniline (P-a) and bisphenol A-aniline-based bifunctional (BA-a) benzoxazines. Due to the introduction of heat-resistant fluorene rings and the increase of crosslinking degree of copolymers, the copolymers (poly(P-a/*t*-BF-sa-a) and poly(BA-a/*t*-BF-sa-a)) showed excellent thermal properties. Among them, the T_g, T_5, T_{10}, and Y_c of poly(P-a/*t*-BF-sa-a) were increased by 34 °C, 58 °C, 35 °C, and 8%, respectively, even higher than that of bisphenol fluorene aniline-based polybenzoxazine. Furthermore, due to the long alkyl chain in the *t*-BF-sa-a monomer, the *E*'of the copolymers was decreased significantly, which greatly improved the shortcomings of traditional polybenzoxazines, such as high brittleness and poor toughness.

1. Introduction

Benzoxazine monomers have some excellent properties, for example, no generation of by-products during the curing process, low porosity, and near-zero shrinkage, etc[1-3]. Therefore, polybenzoxazines have a promising prospect in the application of insulating materials, electronic encapsulating materials, ablative resins, etc [2,4-8]. Benzoxazine monomers have extraordinary molecular design flexibility with different structures, by combining phenols and amines with different structures. This allows the designing of benzoxazine monomer structures with a wide range of properties [9-11]. At present, the reported benzoxazine monomers are mostly bisphenol type and diamine type bifunctional benzoxazine monomers. The studies on the synthesis and properties of asymmetric multi-functional benzoxazine monomers are relatively backward. Moreover, the high curing temperature, poor processability, high brittleness, and poor toughness of polybenzoxazines seriously hinder the further application of such products. Therefore, the preparation of polybenzoxazines with the excellent process and mechanical properties is a hot issue in the applied research.

By introducing some polymerizable groups into the structure of the benzoxazine monomer, the crosslinking density of polybenzoxazine can be effectively increased, and the mechanical properties and thermal stability of the polymer can be significantly improved. Polymerizable groups include allyl, allyl ether, acetylene, propynyl, cyano, norbornene, and maleimide, etc [12-14]. Agag et al. synthesized a series of benzoxazine monomers containing polymerizable groups [15, 16]. The experimental results showed that the thermal properties of the polymers were greatly improved. Later on, Kumar et al. synthesized benzoxazine monomers from the reaction of 2,2'-diallyl-bisphenol-A, aniline, and formaldehyde [17]. The results showed that the T_g of the polymer was 300 °C, and the thermal decomposition temperature of 5% and 10% was as high as 395 and 425 °C, respectively, with excellent thermal performance.

Fluorene-based polymer materials have excellent heat-resistance and flame-retardant properties, high carbon residue rate, limiting oxygen index, light stability, and chemical stability [18-21]. However, fluorene exists in the side chain with the form of overhang in such fluorene-based monomers, which results in the larger rigidity of the polymer segment, the higher curing temperature, and the poor toughness of the

[a] Key Laboratory of Superlight Material and Surface Technology of Ministry of Education, College of Materials Science and Chemical Engineering, Harbin Engineering University, Harbin 150001, China.
[b] Department of Chemical Engineering, Balochistan University of Information Technology, Engineering and Management Sciences, Quetta 87300, Pakistan.
* Corresponding author E-mail:Zhong-cheng Pan (421336390@herbeu.edu.cn), Wen-bin Liu (wjlwb@163.com),Jun Wang (wj6267@sina.com).

View Article Online
DOI: 10.1039/D0NJ04362F

polymer. Consequently, it is essential to redesign the fluorene molecular structure for improving polymer properties [22-26].In this paper, BADHF was prepared via introducing phenolic hydroxyl group and amino group into 2,7,9 positions of fluorene through molecular structure design, using the excellent heat resistance and the active sites of fluorene. The *t-BF-sa-* monomer was synthesized by the o-hydroxy-benzylamine method combined with one-stage Mannich condensation reaction with allylamine as raw material. Compared with the traditional three-step method, the synthesis of asymmetric benzoxazine monomer reduces the treatment process of the intermediate product, and a small amount of sulfuric acid is added into the reaction system to catalyze the reduction of double bonds by sodium borohydride, greatly shortening the reaction time and experimental period, improving the yield of the intermediate product and reducing the production cost. In traditional three-step synthesis method, the double bond reduction process takes 8 to 12 hours, but in this paper, it only takes 15 minutes.

By adjusting the number of rigid and flexible groups and functional groups in benzoxazine monomer, the problems of small molecular weight of the resulting polymers, low crosslinking density, poor toughness, and the decrease of thermal properties due to the introduction of flexible groups can be solved. The typical P-a and BA-a benzoxazine monomers were modified by the prepared polyfunctional fluorenyl benzoxazine monomer, and the influence mechanism of benzoxazine monomer structure on the polymerization behavior and properties of the blends was systematically recognized, which provided a scientific basis for the application of polybenzoxazine in advanced resin matrix composites, ablative materials, electronic packaging materials, and other fields, and promoted the development and perfection of polybenzoxazine application research.

2. Experimental

2.1. Raw materials

2,7-Dihydroxy-fluorene-9-one, o-hydroxybenzaldehyde, and paraformaldehyde were purchased from Kermel Chemical Reagent Co., Ltd. Tianjin, China. Allylamine methylsulfonic acid, trimethylamine, and sodium borohydride were supplied by Jinshan Chemical Reagent Co., Ltd. Chengdu, China. Aniline, concentrated sulfuric acid, ethanol and trichloromethane were purchased from Jingchun Chemical Reagent Co., Ltd. Shanghai, China. The P-a (98.5%) and BA-a (98.0%) monomers were gifted by the Huacui Advanced Materials Co. Ltd. Jiangxi, China.

2.2 Preparation of *t*-BF-sa-a monomer and its intermediates

The synthesis route of *t*-BF-sa-a monomer is shown in **Scheme 1**. The method was discussed in the sub-sections.

2.2.1 Preparation of BADHFmonomer

The BADHF was prepared by the reaction of 2,7-dihydroxy-9-fluorenone with aniline. The followed synthesis method was discussed in detail in an earlier published article [36].

2.2.2 Preparation of reduction products of bisphenol bis amine-salicylaldehyde monomer (*b*-SAH)

BADHF (0.02 mol), concentrated sulfuric acid (0.2 mL), and o-hydroxybenzaldehyde (0.04 mol) were dissolved in 100 mL of ethanol and heated to reflux temperature for 10 h. 0.06 mol of sodium borohydride was added in batches into the mixture after cooling the mixture to room temperature, and then the system was maintained and stirred for another 15 min. Then, dichloromethane was added for extraction, and the organic phase was separated. Finally, the solvent was detached by rotating evaporation, and the intermediate product (*b*-SAH) was obtained with a yield of 78%. FTIR (KBr, cm^{-1}): *v* = 3600-3100 (N–H and O–H stretching overlap), 3032 (unsaturated C-H stretching), 2910 (saturated alkyl C-H stretching), 1368,1338 (CH_2 wagging), 1232 (C–N stretching), 1182 (asymmetric stretching of C–N–C), 950 (out-of-plane C–H). ^{1}HNMR (500 MHz, DMSO-d_6, ppm): 9.45 (s, 2H, –OH), 9.21 (s, 2H, –OH), 6.42-7.44 (m, 22H, Ar–H), 5.88(s, 2H,–NH), 4.11(s, 4H,–CH_2). ^{13}C NMR (100 MHz, DMSO-d_6, ppm): 156.5 (C–OH), 149.8 (C–NH–), 61.2 (the quaternary carbon atom in fluorene ring), 51.6 (Ar–CH_2–N). Elem. Anal. Calcd for $C_{39}H_{32}N_2O_4$: C%: 79.03, H%: 5.44, N%: 4.73. Found: C%: 78.83, H%: 5.58, N%: 4.65.

2.2.3 Preparation of *t*-BF-sa-a monomer

Allylamine (0.01 mol), paraformaldehyde (0.03 mol), *b*-SAH (0.005 mol), and chloroform (50 mL) were stirred into a 250 mL three-necked bottle at 60 °C for 24 h and cooled down to the room temperature. Organic solvents were removed by rotating evaporation, and the crude product was collected. Then it was dissolved in the dichloromethane solvent, and the organic phase was separated by repeated alkali and water washing. Finally, the dichloromethane solvent was removed by rotating evaporation, and t-BF-sa-a was obtained (yield 89%). FTIR (KBr, cm^{-1}): v=3396 (O–H stretching), 3036 (unsaturated C-H stretching), 2847 (saturated alkyl C-H stretching), 1383,1337 (CH_2 wagging), 1251, 1226 (C–O–C asymmetric stretching), 1160 (C–N–C asymmetric stretching), 1113 (C-O-C symmetrical stretching), 928-945 (C–H out-of-plane bending), 1641(C=C stretching of allyl), 990 (=C-H out of plane wagging).^{1}HNMR (500 MHz, *DMSO-d_6*, ppm): 6.41-7.44 (m, 20H, Ar-H), 5.81 (m, 2H, –CH=), 5.81 (m, 4H, =CH_2), 3.35 (s, 4H, –CH_2–), 3.96, 4.58 (s, 8H, Ar–CH2–N), 4.76, 5.36 (s, 8H, O–CH_2–N).^{13}C NMR (100 MHz, *DMSO-d_6*, ppm): 85.6-91.8 (O–CH_2–N), 53.3-58.2 (Ar–CH_2–N), 63.2 (the quaternary carbon atom in fluorene ring), 134.5 (−CH= of allyl), 116.7 (=CH_2 of allyl), 56.3 (−CH_2− of allyl). Elem. Anal. Calcd for $C_{51}H_{46}N_4O_4$: C%: 78.64, H%: 5.95, N%: 7.19. Found: C%: 78.43, H%: 5.68, N%: 7.25.

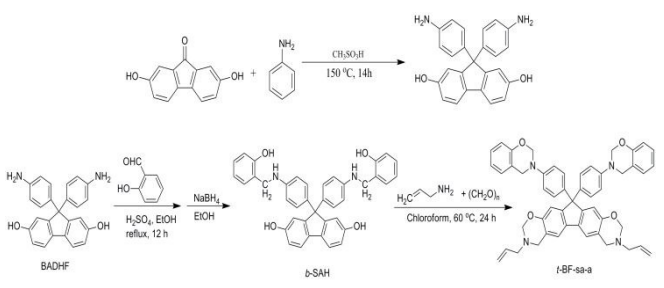

Scheme 1-The synthesizing route of *t*-BF-sa-a monomer

View Article Online
DOI: 10.1039/D0NJ03625

2.3 Curing of *t*-BF-sa-a monomer and copolymers

The *t*-BF-sa-a monomer was added to a definite shape of steel mold and cured in an air-dry oven on isothermal heating at 150, 180, 210, 240, and 260 °C for 2 h at each stage. The BA-a (P-a) and *t-BF-sa-a* monomers with appropriate mass share were mixed by melt blending method on the heating plate and transferred to the steel molds. The mass ratio of BA-a (P-a) and *t-BF-sa-a* monomers was 4:1.The BA-a(P-a)/*t-BF-sa-a* blends were also cured in isothermal heating, following procedure was followed 150 °C/2h + 180 °C/5h + 200 °C/1h + 220 °C/1h.

2.4 Characterization methods

The chemical structures of the *t-BF-sa-a* monomer and its intermediates were confirmed by Fourier transform infrared spectroscopy (FTIR) analysis performed on a Bruker Tensor-27 with KBr disks. Nuclear magnetic resonance spectra of hydrogen and carbon spectrum (^{1}HNMR and ^{13}CNMR) were investigated in *DMSO-d$_6$* solution as a solvent keeping tetramethylsilane as internal standard on a Bruker Avance-III 400 HD spectrometer. Elemental analysis was carried out with a Vario EL cube (Elementar Analysensysteme GmbH). Differential scanning calorimetry (DSC) was studied on a TA Instruments Q200 at a heating rate of 20 °C·min^{-1} from 50 to 400 °C in flowing nitrogen (50 ml·min^{-1}). Thermal-gravimetric analysis (TGA) was employed to evaluate the thermal stability of the polymers, which was carried out from 50 to 800 °C on a TA Instruments Q50 with a heating rate of 10 °C·min^{-1} under the atmosphere of nitrogen. The rheological behaviors were recorded by using a TA Instruments (AR-2000rheometer) with a 25 mm diameter parallel plate fixture at 10 s relaxation time and 3.259 Pa pressure. T_g temperatures of the cured polymers and copolymers were investigated by a dynamic thermal mechanical analyzer (DMA) using dynamic mechanical analyzer TA Q800 at a scanning speed of 5 °C·min^{-1} in a nitrogen atmosphere. The morphological structures of the samples were recorded on a HITACHI S-4300. First, the samples were frozen in liquid nitrogen for a while, then they were taken out and quickly broken; subsequently, the samples adhered to the conductive adhesive keeping cross-section in the upward direction.

3. Results and discussion

3.1 Structural characterization of *t*-BF-sa-a monomer and its intermediates

Figure 1 shows the FTIR spectrum of the *t*-BF-sa-a monomer and its intermediates. For BADHF, the characteristic stretching vibration band of primary amine (-*NH$_2$*) is observed at 3454 cm^{-1}. It can be found that the absorption band at 3381 cm^{-1} is typically for hydroxy (*O-H*) stretching. The characteristic absorption bands at 1611 and 1511 cm^{-1} are corresponding to the benzene ring skeleton. The C-N bending absorption peak can be noticed near 1180 cm^{-1}. However, there is no stretching vibration peak of *C=O* at 1700 cm^{-1}, which indicates that the BADHFhas been successfully synthesized. For *b*-SAH, the *C-N* stretching vibration is observed at 1232 cm^{-1}, while the broadband absorption at 3100-3600 cm^{-1} is designated to the overlapping stretching vibrations of *N-H* and *O-H*. The band at 1232 cm^{-1} is assigned to the stretching vibration of *C-N*. There is no absorption band of C=N vibration near 1615 cm^{-1}, which indicates that the C=N bond has been completely reduced by sodium borohydride. For the *t*-BF-sa-a monomer, it can be seen that the band at 3405 cm^{-1} is the hydroxyl group stretching vibration, which may be caused by the ring-opening of a small number of oxazine rings. The stretching vibration band at 3034 cm^{-1} is attributed to the unsaturated *C-H* in the benzene ring, while the stretching vibration band at 2846 cm^{-1}belongs to the saturated alkyl *C-H*. The bands at 1369 and 1337 cm^{-1} are attributed to the oscillating vibrations of methylene in the oxazine rings. The stretching vibration bands near 1225, 1252, and 1110 cm^{-1} are distributed to the asymmetric and symmetric *C-O-C*, while the stretching vibration of the asymmetric *C-N-C* can be observed at 1158 cm^{-1}. We can notice that the absorption peaks of the oxazine ring appear at 926-944 cm^{-1} corresponding to the out-of-plane bending vibration of *C-H* in the benzene ring. The *C=C* stretching vibration and *=C-H* out-of-plane oscillating vibration peaks of allyl groups are observed at 1641 and 971 cm^{-1}.

Figure 2 shows the ^{1}HNMR spectrum of the intermediates and *t*-BF-sa-a monomer. For BADHF, the hydroxyl proton on the benzene ring is discovered at 9.26 ppm. The chemical shifts at 6.40-7.45 ppm are attributed to the phenyl protons on the benzene rings. The peak at 4.93 ppm is attached to the hydrogen protons on the amino group. For *b*-SAH, the hydroxyl proton on the fluorene ring is observed at 9.45 ppm. The chemical shift at 9.21 ppm represents the hydroxyl protons on the structure of raw material salicylaldehyde. δ=6.42-7.44 ppm are the phenyl protons on the benzene ring. The chemical shift at 5.88 ppm is ascribed to the hydrogen proton of the secondary amine group, and the shift at 4.11 ppm is distributed to the hydrogen protons of the methylene group.

For *t*-BF-sa-a monomer, the 6.41-7.44 ppm are corresponding to hydrogen protons on the benzene ring. The multiple peaks of 5.81 and 5.11 ppm are assigned to hydrogen protons on -*CH=* and *=CH$_2$* of allyl group, and the peak at 3.35 ppm is the hydrogen protons of -*CH$_2$*- of allyl group. The chemical shifts at 3.96 and 4.76 ppm belong to hydrogen protons of *N-CH$_2$*-Ar on the bisphenol oxazine ring, and 4.58 and 5.36 ppm belong to the hydrogen protons of *O-CH$_2$-N* on the diamine oxazine ring.

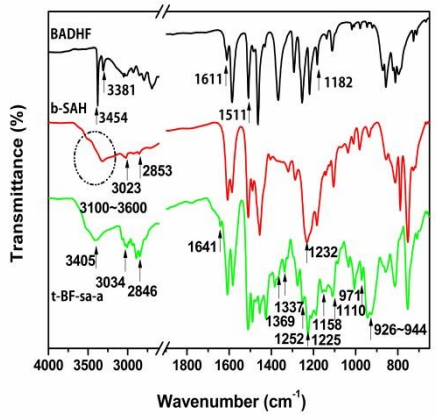

Figure 1-FTIR spectrum of *t*-BF-sa-amonomer along with its intermediates

View Article Online
DOI: 10.1039/D0NJ04262E

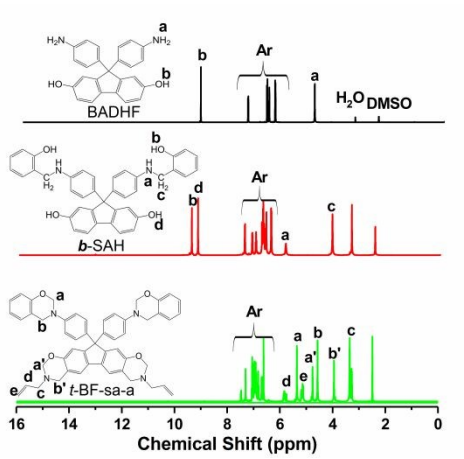

Figure 2-^{1}HNMR spectrum of *t*-BF-sa-a monomer along with its intermediates

In order to further determine the chemical structures of *t*-BF-sa-a monomer and its intermediates, the ^{13}CNMR spectra are shown in **Figure 3**. For BADHF, the single peaks located at 156.5 and 149.8 ppm are assigned to the carbon atom resonances of *C–OH* and *C–NH$_2$*, respectively. The peak around at 61.2 ppm is ascribed to the quaternary carbon atom in fluorene ring. For *b*-SAH, the chemical shift at 51.6 ppm is described to the carbon atom resonances of *Ar–CH$_2$–N* of oxazine ring. The other peaks are similar to that of the BADHF monomer.

For *t*-BF-sa-a monomer, the chemical shifts at 85.6-91.8 and 53.3-58.2 ppm are assigned to the carbon atom resonances of *O–CH$_2$–N* and *Ar–CH$_2$–N* of oxazine ring, respectively. The carbon atom of*–CH$_2$–*on allyl appears at 56.3 ppm, while the carbon atoms of *–CH=* and *=CH$_2$* on allyl are observed at 134.5 and 116.7 ppm, respectively. All expected characteristic absorption peaks were found in the ^{13}CNMR spectra. The spectra data of FTIR, ^{1}HNMR, and ^{13}C NMR show that the *t*-BF-sa-a monomer and its intermediates are synthesized successfully.

3.2 Polymerization behavior of monomer

3.2.1 Rheological properties

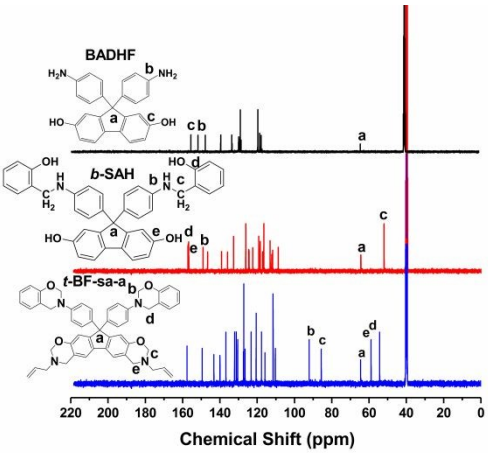

Figure 3-^{13}CNMR spectra of *t*-BF-sa-a monomer and itsintermediates

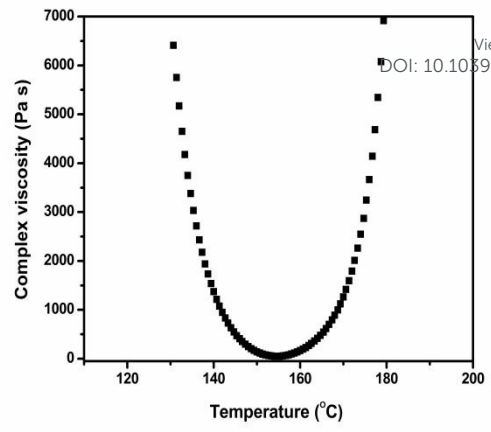

Figure 4-Rheological curve of *t-BF-sa-a* monomer

The study of the rheological properties can provide more intuitive data support and theoretical guidance for the processing and forming process of synthesized benzoxazine monomer. Therefore, for a better understanding of the processing, the rheological behavior of *t*-BF-sa-a monomer was studied by means of temperature scanning. The temperature dependence of the viscosity of *t*-BF-sa-a monomer is performed from 100 to 200 °C and produced as **Figure 4**.

As can be seen from **Figure 4**, the *t*-BF-sa-a monomer is in solid-state at room temperature and begins to melt progressively with increasing temperature, which results in that the molecular motion is enhanced and the system viscosity is reduced obviously. As the temperature is constantly rising, the *t*-BF-sa-a monomer can form a large spatial network structure through the ring-opening polymerization, which limits the molecular movement and increases the viscosity of the system.

In this paper, when the viscosity value is less than 1000 Pa·s, the intersection point of the low-temperature zone is the softening point temperature of the system. The junction point of the high-temperature zone is the gel point temperature of the system, the temperature range between the softening point temperature and the gel point temperature is the processing window temperature of the system [46,47]. The *t*-BF-sa-a monomer has a lower softening point temperature, which is mainly related to the number of aromatic rings and the alkyl chain length. The minimum viscosity of *t*-BF-sa-a monomer was only 66.4 Pa·s. The *t*-BF-sa-a monomer has a lower gel point temperature, which shows that *t*-BF-sa-a monomer can take place the crosslinking reaction at low temperature and has high reactivity.

3.2.2 DSC study on thermal curing behaviour

The curing behavior of *t*-BF-sa-a monomer is determined by DSC analysis after curing on each stage and illustrated as **Figure 5**.

The DSC curve of *t*-BF-sa-a monomer is separately plotted in **Figure 5(A)** for the better visual of readers. There are two exothermic peaks in *t*-BF-sa-a monomer around 230 and 300 °C. There are two reactive groups in *t*-BF-sa-a monomer, i.e. oxazine ring and carbon-carbon double bond in the allyl group. By consulting the relevant literature[49], we infer that

View Article Online
DOI: 10.1039/D0NJ04362F

the extremely strong exothermic peak near 230 °C is the exothermic peak of ring-opening polymerization of the oxazine ring, while the weak exothermic peak at 300 °C is caused by the exothermic polymerization of carbon-carbon double bond in allyl group. The initial temperature of the ring-opening polymerization is 180-190 °C, which indicates that the *t*-BF-sa-a monomer follows the mechanism of 1,3-benzoxazine thermal ring-opening polymerization. From the curve, we can observe that the exothermic enthalpy of the *t*-BF-sa-a monomer is higher, and there is an obvious shoulder peak in the spectrum. This is mainly due to the existence of polymerizable groups in the molecular structure of the *t*-BF-sa-a monomer. At a certain temperature, the *t*-BF-sa-a monomer can undergo addition polymerization, and the addition polymerization peak overlaps partly with the exothermic peak of the ring-opening polymerization. Moreover, the initial curing temperature of the *t*-BF-sa-a monomer is lower, which indicates that the *t*-BF-sa-a monomer has high reactivity.

DSC curves of *t*-BF-sa-a monomer at different curing temperatures are displayed in **Figure 5(B)**. The curing degree of *t*-BF-sa-a monomer at different curing temperatures are 27.8% (at 150 °C), 60.6% (at 180 °C), 79.5% (at 210 °C), 92.9% (at 240 °C), respectively. The curing degree reaches to 27.8% at 150 °C, which can be attributable to the addition reaction mechanism of polymerizable groups. With the increase of curing temperature, the exothermic enthalpy of the *t*-BF-sa-a monomer decreases, and the degree of curing increases, which indicates that the number of unreacted functional groups in the *t*-BF-sa-a monomer is decreased.

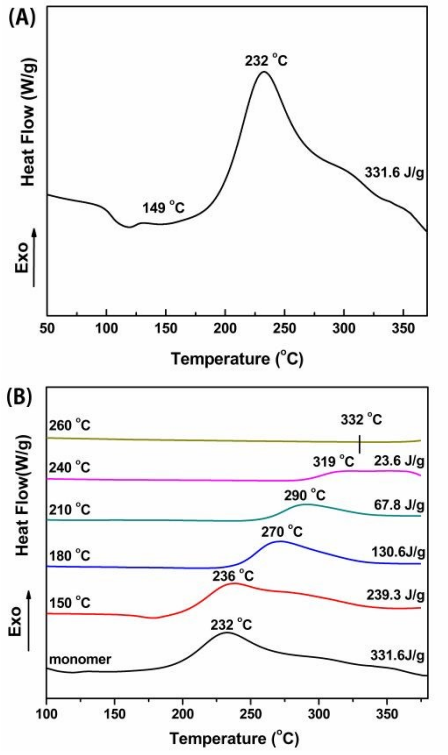

Figure 5-DSC curves of the *t-BF-sa-a* monomer, before curing (A), and after curing at different temperatures (B)

With the curing temperature rising to 260 °C, no exothermic peak is found on the DSC heat flow curve, which indicates that there is no residual uncured benzoxazine group after thermal curing in the *t*-BF-sa-a monomer. Furthermore, with the increase of curing temperature, the peak temperature moves to high temperature in DSC curves. This is because of the increase in curing degree, the more compact crosslinking network hinders the activity of functional groups in the system. Therefore, only by increasing the temperature, the viscosity of the system can be reduced and the reactivity of functional groups can be increased.

3.2.3 FTIR study on thermal curing behavior

FTIR spectrums of *t*-BF-sa-a monomer after curing at different temperatures are exhibited in **Figure 6**.

It can be seen from **Figure6** that, in *t*-BF-sa-a monomer, the peak at 3034 cm^{-1} is attributed to the characteristic absorption of *Ar–OH* formed after the ring-opening of the oxazine ring, which shows that the ring-opening polymerization of oxazine ring with the rupture of *C–O* bond can take place at high temperature. The reaction mechanism of the ring-opening polymerization of the oxazine ring is shown in Scheme 2. The characteristic absorption peaks of the allyl group are located at 1641 cm^{-1} (C=C stretching vibration peak), 971 cm^{-1} (=C-H out-of-plane oscillation vibration peak), and 3082 cm^{-1} (C-H symmetric stretching vibration peak). The decreasing trend of three absorption peaks (1641, 971, and 3082 cm^{-1}) intensities with the increase of curing temperature confirms the participation of the allyl group in the curing reaction [48-50]. The C=C stretching vibration peak of the allyl group disappears completely after curing at 180 °C, which confirms the addition polymerization of the allyl group at this stage. The allyl group reaction mechanism inferred from the test results is shown in Scheme 3.

With the increasing temperature, the oxazine ring characteristic absorption peaks (926-944 cm^{-1}), the rocking vibration absorption peaks of methylene (1369 and 1337 cm^{-1}), C–O–C stretching vibrations (1252 and 1225 cm^{-1}), and C–N–C stretching vibrations (1158 and 1110 cm^{-1}) on the oxazine ring are weakened gradually, and disappear completely after curing on 260 °C. This is due to the addition polymerization of allyl group, increasing the crosslinking density and the system viscosity, and the polymerization process is changed to diffusion control. Therefore, the higher temperature is required for the complete oxazine ring opening. The *t*-BF-sa-a monomer has been completely cured at 260 °C, which is consistent with DSC test results.

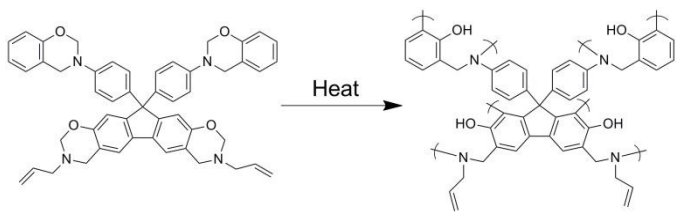

Scheme 2-The reaction mechanism of the ring opening polymerization of oxazine ring

View Article Online
DOI: 10.1039/D0NJ04262E

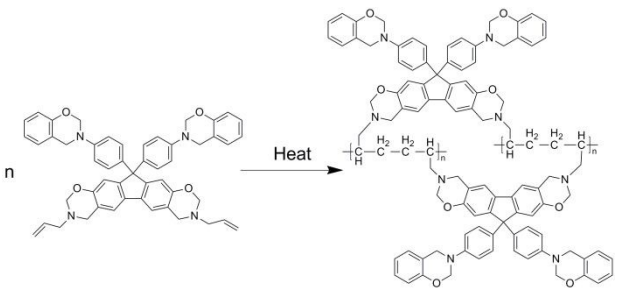

Scheme 3-The reaction mechanism of allyl group

3.3 Thermal and thermomechanical properties

3.3.1 Dynamic mechanical properties

The T_g is a significant parameter to characterize the thermal properties of polymers, and it is the characteristic temperature of polymers from the glass state to the viscoelastic state [37, 38]. In the practical application of polymer materials, the T_g is generally the upper limit of the continuous service temperature for plastics and thermosetting resins, and the lower limit of the continuous service temperature for elastomers [39,40]. The DMA test result of poly(*t*-BF-sa-a) is depicted in **Figure 7**. The rigidity of the material can be directly reflected by the storage modulus, and the damping characteristics of the material can be characterized by the loss factor, and the peak temperature of the loss factor curve is the T_g of the material.

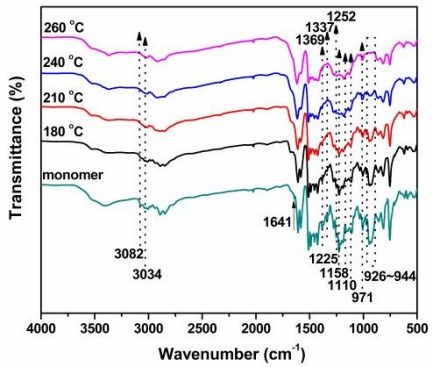

Figure 6-FTIR spectrums of *t*-BF-sa-a monomer after curing at different temperatures

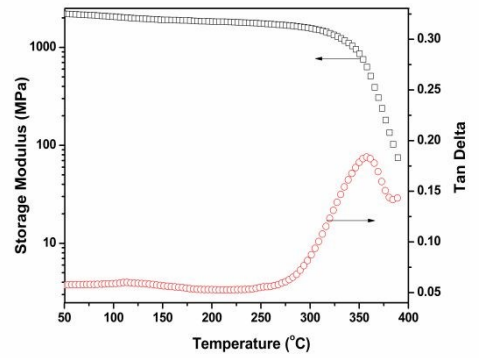

Figure 7-The DMA test results of poly(*t*-BF-sa-a), Storage modulus (A), Loss tangent (B)

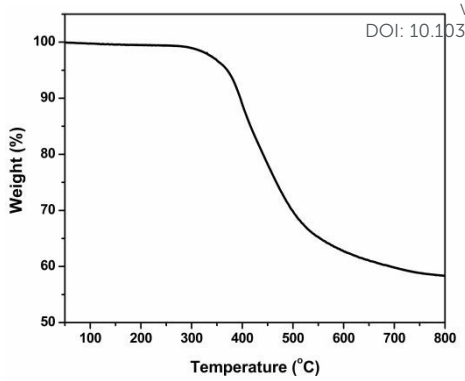

Figure 8-TGA thermograms of poly(*t*-BF-sa-a) in a nitrogen atmosphere

The *tanδ* peak (T_g) of poly(*t*-BF-sa-a) is observed at 356.9 °C, which is much better than that of bisphenol-A-aniline (BA-a) and reported bifunctional fluorenyl polybenzoxazines, showing excellent thermal properties [27-32]. This is because there are abundant intra-and inter-molecular hydrogen bonds in its network structure, the polymer chain is more compact, and the thermal movement of the chain segment is greatly limited. The cross-linking density of poly(*t*-BF-sa-a) is greatly increased due to the existence of polymerizable groups. The introduction of fluorenyl group can increase the rigidity of the molecular chain, limit the internal rotation of the polymer chain. In addition, poly(*t*-BF-sa-a) exhibits a high storage modulus (*E'*), as high as 2200MPa in the glassy state. This is mainly because the introduction of polymerizable groups in the monomer structure increases the cross-linking density of the polymer, which makes the polymer segments begin to move at a higher temperature.

3.3.2 Thermal stability

The thermogravimetric curve of poly(*t*-BF-sa-a) in a nitrogen environment is displayed in **Figure 8**. The initial degradation temperatures (T_5 and T_{10}) of poly(*t*-BF-sa-a) are recorded at 370 °C and 396 °C, respectively, and the carbon residue (Y_c) at 800 °C is 58.4%, which are higher than that of bisphenol fluorene aniline-based polybenzoxazine [28,33-35,45].

This is because the increase of the number of oxazine rings can improve the crosslinking density of the polymer, and the increase of the number of aromatic rings will lead to the high carbon residue rate of the polymer. The introduction of large volume rigid fluorene ring can effectively improve the heat resistance of the polymer, and the increase of the number of functionalities can also improve the cross-linking density of the poly(*t*-BF-sa-a), effectively reduce the number of unstable end groups in the polymer, so as to improve the thermal stability of the polymer. The *t*-BF-sa-a monomer contains the polymerizable allyl groups. The additive polymerization of allyl groups can further improve the crosslinking density and prevent the volatilization of amine during the initial thermal decomposition stage.

3.4 Copolymerization with traditional benzoxazine monomers

Traditional monofunctional P-a benzoxazine and bifunctional BA-a benzoxazine have excellent processing performance, but they also have some disadvantages such as high brittleness,

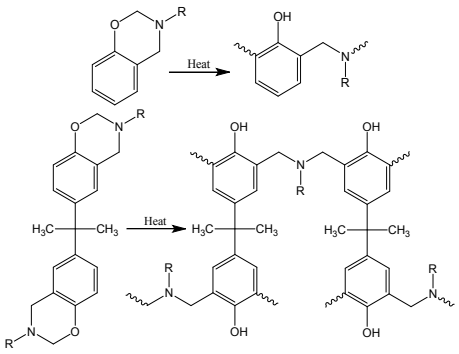

Scheme 4-Polymerization reaction of P-a and BA-a

poor toughness, low thermal performance, and poor thermal stability [41, 42]. P-a monomer and BA-a monomer can undergo the ring-opening polymerization on heating and form linearcross-linking structure, and their structures are similar to that of phenolic resins [42,43]. The polymerization process is shown in **Scheme 4**.

The processing properties, thermal stabilities, and mechanical properties of fluorenyl polybenzoxazines can be improved and enhanced by adjusting the ratio of rigid and flexible groups and introducing other functional groups [44]. However, the introduction of large structure of fluorenyl ring still leads to the shortcomings such as low cross-linking density, high brittleness, and high synthesis cost [45]. Therefore, it is an economical and effective method to modify traditional benzoxazines by blending or copolymerization, and to improve the comprehensive properties of resin materials by using synthesized high-performance monomers. The synthesized *t*-BF-sa-a monomer can form a highly crosslinked polymer network structure after the ring-opening polymerization. This is due to the fact that the existence of more cross-linking sites and active functional groups in the monomer structure can greatly affect the properties of traditional polybenzoxazines (poly(P-A) and poly(BA-a)).

3.4.1DSC of P-a/*t*-BF-sa-a and BA-a/t-BF-sa-ablends

The DSC curves of neat P-a and BA-a monomer, P-a/*t*-BF-sa-a blends and BA-a/*t*-BF-sa-a blends are shown in **Figure 9**.

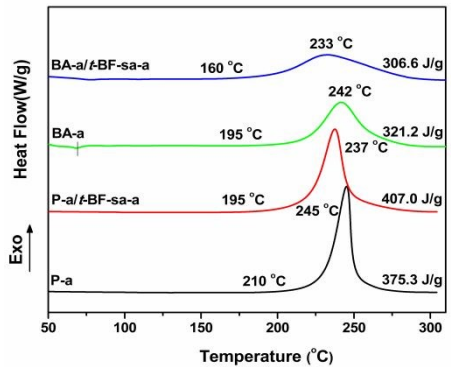

Figure 9-DSC spectra of neat P-a and BA-a, and P-a/*t*-BF-sa-a and BA-a/*t*-BF-sa-ablends

It can be seen from Figure 9 that there is a sharp exothermic peak in P-a monomer and P-a/*t*-BF-sa-a blends, which corresponds to the ring-opening polymerization of the reaction system. The initial polymerization temperature of P-a monomer is 210 °C, the maximum exothermic peak temperature is 245 °C, and the polymerization enthalpy is 375.3 J/g. When *t*-BF-sa-a monomer is added into P-a monomer, the initial polymerization temperature and the peak temperature of the P-a/*t*-BF-sa-a blends are decreased from 210 °C and 245 °C to 195 °C and 237 °C, respectively, but the exothermic enthalpy is increased. This is related to the lower initial polymerization temperature of *t*-BF-sa-a monomer. When *t*-BF-sa-a monomer is added into P-a monomer, the thermal ring-opening polymerization of *t*-BF-sa-a monomer in the P-a/*t*-BF-sa-a blends will take place in advance, and the phenol hydroxyl with catalytic activity will be produced, and then the thermal ring-opening polymerization of P-a monomer is initiated. In addition, due to the presence of polymerizable group in *t*-BF-sa-a monomer, there are more crosslinking sites in *t*-BF-sa-a monomer, which results in a higher exothermic enthalpy of the P-a/*t*-BF-sa-a blends than that of P-a monomer.

When *t*-BF-sa-a monomer is added into BA-a monomer, the initial polymerization temperature of the BA-a/*t*-BF-sa-a blends is significantly decreased. This is because BA-a monomer is solid at room temperature (melting point: 69 °C). When the addition reaction of allyl group in *t*-BF-sa-a monomer takes place, the amount of flexible alkyl in the BA-a/*t*-BF-sa-a blends increases, which results in the molecular flexibility of the BA-a/*t*-BF-sa-a blends increases, the collision and transfer of functional groups becomes much easier, the polymerization activity increases, and the initial polymerization temperature decreases.

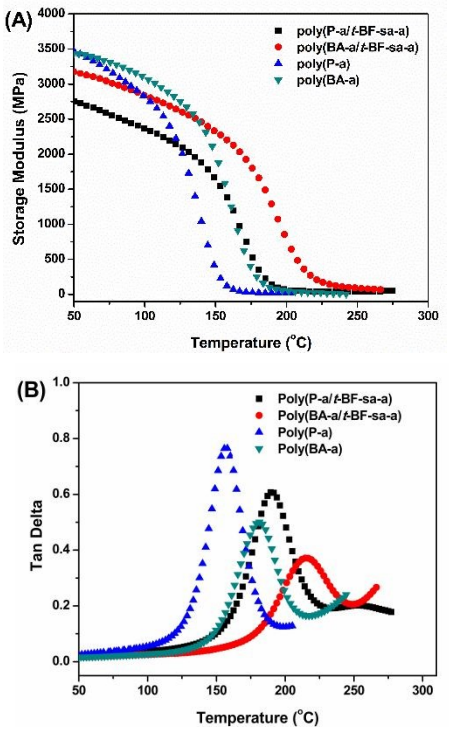

Figure 10-The DMA test results of neat and copolymers

View Article Online
DOI: 10.1039/D0NJ04262E

Table1-DMA analysis of neat and copolymers

Samples	T_g (°C)	E' (MPa, 50 °C)	Crosslinking Density(mol·cm^{-3})
Poly(P-a)	157.1	3478	0.00415
Poly(P-a/*t*-BF-sa-a)	190.4	2743	0.00566
Poly(BA-a)	181.2	3440	0.00479
Poly(BA-a/*t*-BF-sa-a)	215.5	3178	0.00699

3.4.2 Dynamic mechanical properties of copolymers

The DMA test results of poly(P-a), poly(BA-a), poly(P-a/*t*-BF-sa-a), and poly(BA-a/*t*-BF-sa-a) are shown in **Figure 10**, and the dynamic mechanical property parameters are shown in **Table 1**. When *t*-BF-sa-a monomer is added into P-a monomer, the T_g of poly(P-a/*t*-BF-sa-a) is increased from 157.1 °C to 190.4 °C. This is related to the introduction of heat-resistant fluorene group and increases the crosslinking degree of poly(P-a/*t*-BF-sa-a). The *t*-BF-sa-a monomer contains a large number of polymerizable groups, which can significantly increase the crosslinking density, so poly(P-a/*t*-BF-sa-a) shows excellent thermoproperties. However, compared with poly(P-a), the *E*' of poly(P-a/t-BF-sa-a) is decreased. This is due to the fact that *t*-BF-sa-a monomer has flexible long chain alkyl. The flexibility of polymer chain segment is enhanced, which leads to the decrease of *E'* and the improvement of thermomechanical properties of poly(P-a/*t*-BF-sa-a). This also is mainly due to the formation of aliphatic chains after the addition polymerization of allyl, which increases the flexibility of molecular chains.

It can be seen from the figure that when *t*-BF-sa-a monomer is added into BA-a monomer, the T_g of poly(BA-a/*t*-BF-sa-a) also increases obviously, and the *E'* decreases, which is the same as that of P-a monomer modified by *t*-BF-sa-a monomer. The T_g of poly(BA-a/*t*-BF-sa-a) is increased 34.3 °C compared with that of poly(BA-a).This is related to the structure of BA-a monomer. The structure of bifunctional BA-a monomer is close to that of *t*-BF-sa-a monomer, so they can be copolymerized well, which makes the cross-linking network of poly(BA-a/*t*-BF-sa-a) more compact.

The crosslinking density was calculated by using the derived equation of statistical theory of rubber elasticity by Nielsen[53].

$$log_{10}(E'_e) = 7 + 293 \times (\rho_x)$$

Table2-Summary of the thermal stability parameters of neat and copolymers

Sample	T_5 (°C)	T_{10} (°C)	Y_c (%, 800°C)
Poly(P-a)	280	335	36.7
Poly(P-a/*t*-BF-sa-a)	338	370	44.7
Poly(BA-a)	316	336	28.1
Poly(BA-a/*t*-BF-sa-a)	331	361	40.8

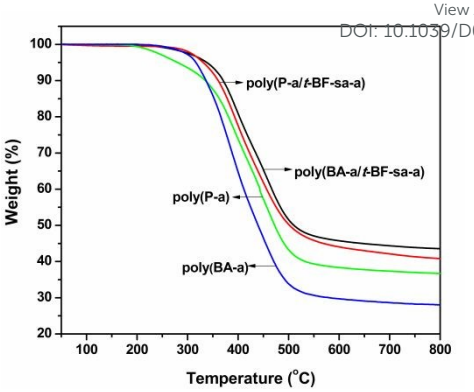

Figure 11-TGA thermograms of poly(P-a), poly(BA-a), poly(P-a/*t*-BF-sa-a), and poly(BA-a/*t*-BF-sa-a)

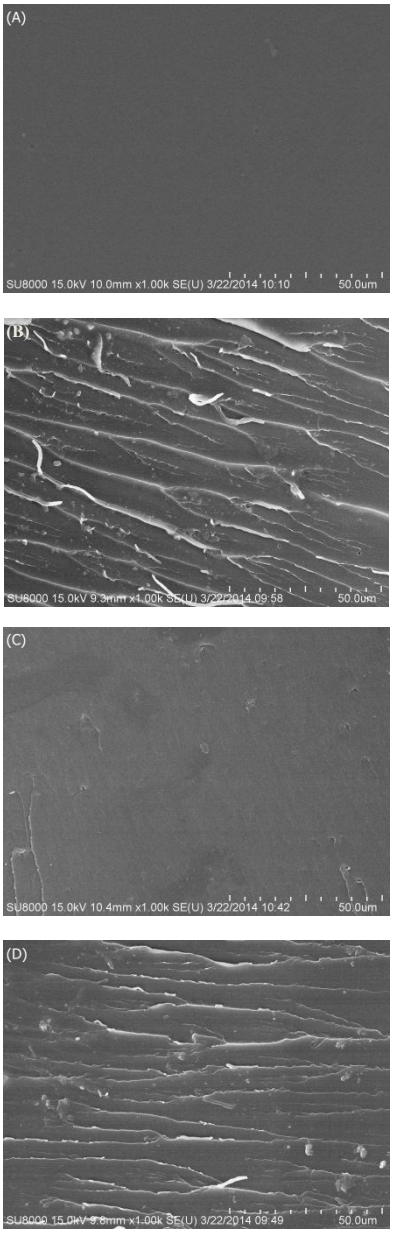

Figure 12-SEM micrographs of the neat and copolymer resins, poly(P-a) (A),poly(P-a/*t*-BF-sa-a)(B), poly(BA-a) (C), and poly(BA-a/*t*-BF-sa-a) (D)

Where E_e' in (dyn·cm^{-2}) is the equilibrium storage modulus measured at (T_g + 40°C) and ρ_x is the cross linking density (mol·cm^{-3}).The crosslinking densities of both copolymers were increased due to the copolymerization reaction between two monomers. The crosslinking of oxazine rings and allyl groups in two monomers improved the crosslinking densities of the copolymers from 0.00415 mol·cm^{-3} [poly(P-a)] and 0.00479 mol·cm^{-3} [poly(BA-a)] to 0.00566 mol·cm^{-3} [Poly(P-a/t-BF-sa-a)] and 0.00699 mol·cm^{-3} [Poly(BA-a/t-BF-sa-a)], respectively, which confirms the enhancement in the macromolecule segments formation in the copolymer [54].

3.4.3 Thermal stability of copolymers

The TGA test results of poly(P-a), poly(BA-a), poly(P-a/*t*-BF-sa-a), and poly(BA-a/*t*-BF-sa-a) are displayed in **Figure 11**, and extracted data are summarized in **Table 2**.

We can easily observe that the initial thermal decomposition temperatures (T_5 and T_{10}) of poly(P-a/*t*-BF-sa-a) are 338 °C and 370 °C, respectively, and the carbon residue rate (Y_c) is 44.7% at 800 °C, which is 58 °C, 35 °C, and 8% higher than that of poly(P-a), even higher than that of bisphenol fluorene-aniline-based polybenzoxazine. This is mainly due to the addition of *t*-BF-sa-a can improve the crosslinking density and the thermal stability of the molecular chain of poly(P-a/*t*-BF-sa-a), and prevent the volatilization of unstable components in the network structure.

The T_5, T_{10}, and Y_c for poly(BA-a/*t*-BF-sa-a) are recorded as 331 °C, 361 °C, and 40.8%, respectively, which are also higher than that of poly(BA-a). This is due to the introduction of rigid fluorene ring and polymerizable group in *t*-BF-sa-a monomer, which results in the increase of the crosslinking density and molecular chain rigidity of the copolymer. And it is easier to form carbon deposition, so it has excellent thermal properties.

3.4.4 Morphology of copolymers

The fracture morphologies of pristine poly(P-a) and poly(BA-a), poly(P-a/*t*-BF-sa-a) and poly(BA-a/*t*-BF-sa-a) copolymers are depicted in **Figure 12**.

The fracture surface of poly(P-a) is smooth and flat, and shows low toughness. However, when *t*-BF-sa-a monomer was added, the cross-section structure of poly(P-a/*t*-BF-sa-a) was rough. This is because the crosslinking degree of the copolymer increases with the addition of *t*-BF-sa-a monomer, and the high crosslinking network structure can prevent the sample from fracture under external force, so the fracture occurs after a lot of deformation. The fracture surface of poly(P-a/*t*-BF-sa-a) presents uniform dendritic folds, and the number of creases is larger, showing obvious ductile fracture characteristics [52], which indicates that the toughness of the copolymer has been significantly improved. The addition polymerization of the allyl group in *t*-BF-sa-a monomer results in the formation of aliphatic chains, which can increase the flexibility of molecular chains and show tough fracture. For poly(P-a/*t*-BF-sa-a), the impact energy from the outside can not only be absorbed or buffered, but also the direction of stress propagation can be prevented or changed due to the increase of flexible polymer segments so that the mechanical properties can be improved [51]. Similarly, the poly(BA-a) and its copolymer showed a similar cross-sectional morphology and homogeneous structure with no obvious defects.

Conclusions

The curing reaction of *t*-BF-sa-a follows the thermal ring-opening polymerization of 1,3-benzoxazine. The introduction of fluorene ring in the polymer network structure improves the rigidity of the molecular chain and limits the thermal movement and internal rotation of the polymer chain segment. With the increase of the number of oxazine ring and polymerizable group, the crosslinking density of the polymer is increased and the network structure becomes more compact. Therefore, the poly(*t*-BF-sa-a) displays a higher T_g and thermal stability than those of the corresponding bifunctional fluorene-based polybenzoxazines. In the meantime, *t*-BF-sa-a monomer shows low melting point and good processing property. DSC, DMA and TGA are used to study the polymerization behavior, thermal properties and thermomechanical properties of poly(P-a/*t*-BF-sa-a) and poly(BA-a/*t*-BF-sa-a), and their cross-section morphologies are observed by SEM. The results indicate that *t*-BF-sa-a can copolymerize with P-a and BA-a. Under the catalysis of *t*-BF-sa-a monomer, the initial exothermic temperature and peak temperature of BA-a/*t*-BF-sa-a blends are significantly reduced, show a significant catalytic activity. The T_g*s* and thermal stabilities of the copolymers are improved obviously due to the introduction of fluorene ring and allyl group and the increase of network structure crosslinking degree. In addition, due to *t*-BF-sa-a monomer contains a long alkyl chain, the *E'* values of the copolymers are decreased significantly. The cross sections of the copolymers show uniform and disordered dimples or treelike fold, and show obvious ductile fracture characteristics, which indicates that the introduction of allyl group into the copolymer network structure has obvious toughening effect.

Conflicts of interest

There are no conflicts to declare.

Acknowledgements

Funding: This work was supported by the National Natural Science Foundation of China [grant number 51773048]; the Natural Science Foundation of Heilongjiang Province [grant number E2017022]; and the Fundamental Research Funds for the Central Universities [grant number HEUCFP201724].

References

1 B. Xue and X.L. Zhang, Modern application and development trend of phenolic resin, *Thermosetting resin*, 2007, **22**(4), 47-50.

2 X. Ning and H. Ishida, Phenolic materials via ring-opening polymerization: Synthesis and characterization of bisphenol-A based benzoxazines and their polymers, *Journal of Polymer Science Part A: Polymer Chemistry*, 1994, **32**(6), 1121-1129.

3 X. Ning and H. Ishida, Phenolic materials via ring-opening polymerization of benzoxazines: Effect of molecular structureon mechanical and dynamic mechanical properties, *Journal of Polymer Science Part B: Polymer Physics*, 1994, **32**(5), 921-927.

4 N.N. Ghosh, B. Kiskan and Y. Yagci, Polybenzoxazines-New high performance thermosetting resins: Synthesis and properties, *Progress in Polymer Science*, 2007, **32**(11), 1344-1391.

5 D.R. Yei, H.K. Fu, W.Y. Chen, et al., Synthesis of a novel benzoxazine monomer-intercalated montmorillonite and the curing kinetics of polybenzoxazine/clay hybrid nanocomposites, *Journal of Polymer Science Part B: Polymer Physics*, 2006, **44**(2), 347-358.

6 C. Jubsilp, K. Punson, T. Takeichi, et al., Curing kinetics of Benzoxazine–epoxy copolymer investigated by non-isothermal differential scanning calorimetry, *Polymer Degradation and Stability*, 2010, **95**(6), 918-924.

7 J. Wang, X. Fang, M.Q. Wu, et al., Synthesis, curing kinetics and thermal properties of bisphenol-AP-based benzoxazine, *European Polymer Journal*, 2011, **47**(11), 2158-2168.

8 J. Wang, H. Wang, J.T. Liu, et al., Synthesis, curing kinetics and thermal properties of novel difunctional chiral and achiral benzoxazines with double chiral centers, *Journal of Thermal Analysis and Calorimetry*, 2013, **114**(3), 1255-1264.

9 D. Yu, H. Chen, Z. Shi, et al., Curing kinetics of benzoxazine resin by torsional braid analysis, *Polymer*, 2002, **43**(11), 3163-3168.

10 P. Kasemsiri, S. Hiziroglu and S. Rimdusit, Effect of cashew nut shell liquid on gelation, cure kinetics, and thermomechanical properties of benzoxazine resin, *Thermochimica Acta*, 2011, **520**(1-2), 84-92.

11 W.S. Chow, S. Grishchuk, T. Burkhart, et al., Gelling and curing behaviors of benzoxazine/epoxy formulations containing 4,4′-thiodiphenol accelerator, *Thermochimica Acta*, 2012, **543**(0), 172-177.

12 Y. Liu, Z. Yue and J. Gao, Synthesis, characterization, and thermally activated polymerization behavior of bisphenol-S/aniline based benzoxazine, *Polymer*, 2010, **51**(16), 3722-3729.

13 C. Andronescu, S.A. Garea, C. Deleanu, et al., Characterization and curing kinetics of new benzoxazine monomer based on aromatic diamines, *Thermochimica Acta*, 2012, **530**(0), 42-51.

14 B. Kiskan, Adapting benzoxazine chemistry for unconventional applications, *Reactive and Functional Polymers*, 2018, **129**, 76-88.

15 T. Agag and T. Takeichi, Novel Benzoxazine Monomers Containing p-Phenyl Propargyl Ether: Polymerization of Monomers and Properties of Polybenzoxazines, *Macromolecules*, 2001, **34**(21), 7257-7263.

16 T. Agag and T. Takeichi, Synthesis and Characterization of Novel Benzoxazine Monomers Containing Allyl Groups and Their High Performance Thermosets, *Macromolecules*, 2003, **36**(16), 6010-6017.

17 K.S. Santhosh Kumar, C.P. Reghunadhan Nair, T.S. Radhakrishnan, et al., Bis allyl benzoxazine: Synthesis, polymerization and polymer properties, *European Polymer Journal*, 2007, **43**(6), 2504-2514.

18 H.J. Kim, Z. Brunovska, H. Ishida, Molecular characterization of the polymerization of acetylene-functional benzoxazine resins, *Polymer*, 1999, **40**(7), 1815-1822.

19 T. Wang, X.Y. He, A.Q. Dayo, et al., Synthesis of novel multi-functional fluorene-based benzoxazine resins: polymerization behaviour, curing kinetics, and thermal properties, *Reactive and Functional Polymers*, 2019, **143**, 104344.

20 C.A. Terraza, J.G. Liu, Y.N. akamura, et al., Synthesis and properties of highly refractive polyimides derived from fluorene-bridged sulfur-containing dianhydrides and diamines, *Journal of Polymer Science Part A: Polymer Chemistry*, 2008, **46**(4), 1510-1520.

21 C. Wang, X. Zhao, G. Li, et al., Novel fluorinated polyimides derived from 9,9-bis(4-amino-3,5-difluorophenyl)fluorene and aromatic dianhydrides, *Polymer Degradation and Stability*, 2009, **94**(10), 1746-1753.

22 C.P. Yang and J.H. Lin., Syntheses and properties of aromatic polyamides and polyimides derived from 9,9-bis[4-(p-aminophenoxy)phenyl] fluorene, *Journal of Polymer Science Part A: Polymer Chemistry*, 1993, **31**(8), 2153-2163.

23 Y.L. Kobzar, I.M. Tkachenko, V.N. Bliznyuk, et al., Fluorinated polybenzoxazines as advanced phenolic resins for leading-edge applications, *Reactive and Functional Polymers*, 2018, **133**, 71-92.

24 S.H. Hsiaoand, C.T. Li, Synthesis and characterization of new fluorene-based poly(ether imide)s, *Journal of Polymer Science Part A: Polymer Chemistry*, 1999, **37**(10), 1403-1412.

25 Y. Lu, M.M. Li, Y.J. Zhang, et al., Synthesis and curing kinetics of benzoxazine containing fluorene and furan groups, *Thermochimica Acta*, 2011, **515**(1-2), 32-37.

26 Y.P. Chen, A.Q. Dayo, H.Y. Zhang, et al., Synthesis of cardanol-based phthalonitrile monomer and its copolymerization with phenol–aniline-based benzoxazine, *Journal of Applied Polymer Science*, 2019, **136**(20), 47505.

27 W. Liu, Q. Qiu, J. Wang, et al., Curing kinetics and properties of epoxy resin–fluorenyl diamine systems, *Polymer*, 2008, **49**(20), 4399-4405.

28 A.Q. Dayo, S. Ullah, J. Kiran, et al., Tensile and water absorption behaviour of polybenzoxazine/hemp fibres composites: Experimental analysis and theoretical validation, *Digest Journal of Nanomaterials and Biostructures*, 2019, **14**(1), 231-241.

29 J. Wang, X.Y. He, J.T. Liu, et al., Investigation of the Polymerization Behavior and Regioselectivity of Fluorene Diamine-Based Benzoxazines, *Macromolecular Chemistry and Physics*, 2013, **214**(5), 617-628.

30 X.Y. He, J. Wang, N. Ramdani, et al., Investigation of synthesis, thermal properties and curing kinetics of fluorene diamine-based benzoxazine by using two curing kinetic methods,*Thermochimica Acta*, 2013, **564**(0), 51-58.

31 X.Y. He, J. Wang, Y.D. Wang, et al., Synthesis, thermal properties and curing kinetics of fluorene diamine-based benzoxazine containing ester groups, *European Polymer Journal*, 2013, **49**(9), 2759-2768.

32 J. Wang, T.T. Ren, Y.D. Wang, et al., Synthesis, curing behavior and thermal properties of fluorene-containing benzoxazines based on linear and branched butylamines, *Reactive and Functional Polymers*, 2014, **74**(0), 22-30.

33 J. Wang, M.Q. Wu, W.B. Liu, et al., Synthesis, curing behavior and thermal properties of fluorene containing benzoxazines, *European Polymer Journal*, 2010, **46**(5), 1024-1031.

34 J. Wang, M.Q. Wu and W.B. Liu, Synthesis and thermal properties of fluorenyl benzoxazine monomers, *Journal of Hunan University*, 2010, **37**(6), 67-70.

35 K. Zhang, L. Han, P. Froirnowicz, et al., Synthesis, polymerization kinetics and thermal properties of para-methylol functional benzoxazine, *Reactive and Functional Polymers*, 2018, **129**, 23-28.

36 H. Wang, J. Wang, X.Y. He, et al., Synthesis of novel furan-containing tetrafunctional fluorene-based benzoxazine monomer and its high performance thermoset, *RSC Advances*, 2014, **4**(110), 64798–64801.

37 M.T. Kalichevsky, E.M. Jaroszkiewicz, S. Ablett, et al., The glass transition of amylopectin measured by DSC, DMTA and NMR, Carbohydrate Polymers, 1992, **18**(2), 77-88.

38 R.R. Ruan, Z. Long, A. Song, et al., Determination of the Glass Transition Temperature of Food Polymers Using Low Field NMR, *LWT-Food Science and Technology*, 1998, **31**(6), 516-521.

NEW JOURNAL OF CHEMISTRY ARTICLE

View Article Online
DOI: 10.1039/D0NJ04262E

39 M. Yazdi, P. Lee-Sullivan, Determination of dual glass transition temperatures of a PC/ABS blend using two TMA modes, *Journal of Thermal Analysis and Calorimetry*, 2009, **96**(1), 7-14.
40 M.S. Rahman, I.M. Al-Marhubi, A. Al-Mahrouqi, Measurement of glass transition temperature by mechanical (DMTA), thermal (DSC and MDSC), water diffusion and density methods: A comparison study, *Chemical Physics Letters,* 2007, **440**(4-6), 372-377.
41 A.Q. Dayo, X.M. Cao, W.A. Cai, et al., Synthesis of benzophenone-center bisphenol-A containing phthalonitrilemonomer (BBaph) and its copolymerization with P-a benzoxazine, *Reactive and Functional Polymers*, 2018, **129**, 46–52.
42 D. Lv, A.Q. Dayo, A.R. Wang, et al., Curing behavior and properties of benzoxazine-co-self-promotedphthalonitrile polymers, *Journal of Applied Polymer Science,* 2018, **135**.
43 H.A. Ghouti, A. Zegaoui, M. Derradji, et al.,Multifunctional hybrid composites with enhanced mechanical and thermal propertiesbased on polybenzoxazine and chopped kevlar/carbon hybrid fibers, *Polymers*, 2018, **10**, 1308.
44 J. Wang, M.Q.Wu, W.B.Liu, et al., Synthesis, curing behavior and thermal properties of fluorene containing benzoxazines, *European Polymer Journal*, 2010, **46**(5), 1024-1031.
45 Y.L. Liu, C.Y. Chang, C.Y. Hsu, et al., Preparation, characterization, and properties of fluorene-containing benzoxazine and its corresponding cross-linked polymer, *Journal of Polymer Science Part A: Polymer Chemistry*, 2010, **48**(18), 4020-4026.
46 S. Rimdusit, P. Kunopast, and I. Dueramae, Thermomechanical properties of arylamine-based benzoxazineresins alloyed with epoxy resin. *Polymer Engineering & Science*, 2011, **51**(9), 1797-1807.
47 C. Jubsilp, T. Takeichi, and S. Rimdusit, Effect of novel benzoxazine reactive diluent on processability and thermomechanical characteristics of bi-functional polybenzoxazine. *Journal of Applied Polymer Science*, 2007, **104**(5), 2928-2938.
48 T.M. Keller and J.R. Griffith, The Synthesis of a New Class of Polyphthalocyanine Resins.*Rights& Permissions*, 1980, **3**,25-34.
49 K.S.S. Kumar, C.P.R. Nair, T.S. Radhakrishnan, and K.N. Ninan, Bis Allyl Benzoxazine:Synthesis, Polymerisation and Polymer Properties. *European Polymer Journal*, 2007, **43**(6), 2504-2514.
50 G.P. Cao, W.J. Chen, and X.B. Liu, Synthesis and Thermal Properties of the Thermosetting ResinBased on Cyano Functionalized Benzoxazine. *Polymer Degradation and Stability*, 2008, **93**, 739-744.
51 X. Zhao, H. Guo, Y.J. Lei, et al. Effect of polyarylene ether nitriles on processing and mechanical behaviors of phthalonitrile-epoxy copolymers and glass fiber laminated composites. *Journal of Applied Polymer Science*, 2013, **6**(127), 4873-4878.
52 Z.R. Chen, Y.J. Lei, H.L. Tang, et al. Mechanical, thermal, electrical and interfacial properties of high performance bisphthalonitrile/polyarylene ether nitrile/glass fiber composite laminates. *Polymer Composites*, 2013, **12**(34), 2160-2168.
53 L. E. Nielsen, Cross-Linking-Effect onPhysical Properties of Polymers. *Journal of Macromolecular Science, Part C*, 1969, **3**, 69-103.
54 R. He, X.L. Zhan, Q.H. Zhang, F.Q. Chen, Toughening of polyamide-6 with little loss in modulus by block copolymer containing poly(styrene-alt-maleic acid) segment, *Journal of Applied Polymer Science*, 2017, **134**, 44849.